Vietnam Journal of Mechanics, Vol. 44, No. 4 (2022), pp. 490 – 499
DOI: https://doi.org/10.15625/0866-7136/17948

RESPONSE ANALYSIS OF UNDAMPED PRIMARY SYSTEM SUBJECTED TO BASE EXCITATION WITH A DYNAMIC VIBRATION ABSORBER INTEGRATED WITH A PIEZOELECTRIC STACK ENERGY HARVESTER

N. N. Linh[1], **V. A. Tuan**[2], **N. V. Man**[2], **N. D. Anh**[3]
[1]*Thuyloi University, Hanoi, Vietnam*
[2]*Hanoi University of Civil Engineering, Hanoi, Vietnam*
[3]*Institute of Mechanics, VAST, Hanoi, Vietnam*
[*]E-mail: tuanva3@huce.edu.vn

Received: 10 December 2022 / Published online: 30 December 2022

Abstract. Dynamic vibration absorber (DVA) integrated with a piezoelectric stack energy harvesting subjected to base excitation is introduced in this paper. The system of dynamic vibration absorber and piezoelectric stack energy harvesting system (DVA-PSEH) has two functions, the first is to reduce vibrations for the primary system, and the second is to convert a part of the vibrational energy into electricity through the piezoelectric effect. The mechanical and electrical responses of the electromechanical system are determined by the complex amplitude method, then the numerical simulations are carried out to investigate the characteristics of DVA-PSEH.

Keywords: dynamic vibration absorber, vibration energy harvesting, piezoelectric stack.

1. INTRODUCTION

In the past few decades, the research in the field of energy harvesting from available energy sources in the surrounding environment, such as vibration, heat, light, radiation, wind and water, into energy the amount of electricity that replaces the use of grid electricity or batteries for low-power electronic devices used in sensors or measuring devices used in vehicles, construction equipment or artificial biological components has received the attention of many researchers. One of the sources of wasted energy that can be harvested for a variety of applications is vibrations from the surrounding environment.

Many designs and approaches have been proposed to convert mechanical energy from vibrational sources in the environment to electrical energy for small and micropower electronic devices such as electromagnetic, piezoelectric, electrostatic, magnetostriction, and triboelectric. Prominent among them is the piezoelectric mechanism, which has

a wide range of applications, from piezoelectric energy harvester (PEH) devices to sensors or actuators.

According to the direction of deformation and electric field of piezoelectric materials, piezoelectric energy harvesters are designed in two basic forms which are horizontal type (piezoelectric cantilever beam) and vertical type (piezoelectric stack) [1]. The piezoelectric stack energy harvester (PSEH) is composed of several layers of piezoelectric ceramics installed in series, with electrodes interspersed between them, which are connected to an external resistor. For this reason, PSEH reduces the distance between electrodes and thereby increases the efficiency of energy harvesting when subjected to mechanical deformation compared to a piezoelectric block of the same size [2]. Besides, PSEH is also capable of withstanding large loads, so it can be applied to large structural objects. Some typical applications of PSEH developed from 2010 onwards can be mentioned as integration with backpacks [3], footwear [4], traffic-induced pavement [5] the suspension system of the vehicle [6,7], railway [8], tuned mass damper [9]

For the system subjected to base excitation, the studies on energy harvesting using piezoelectric stack harvesters are very few and mainly focus on the suspension system. Hendrowati et al. [6] performed a study on an energy harvesting device from the vibration of two-degree-of-freedom suspension subjected to harmonic excitation by applying a single-degree-of-freedom mathematical model of a multilayer piezoelectric vibration energy harvesting mechanism (ML PZT VEH) using the principle of force amplification, then using Laplace transform and simulation on Matlab Simulink software to determine the necessary parameters of the system. The authors also showed that mounting ML PZT VEH does not change the performance of the suspension. Daraseb et al. [7] built a mathematical model of quarter-car and half-car models with a built-in piezoelectric stack which was installed in series with the suspension spring to maintain the operation of the car compared to the original. The harvested voltage and power are theoretically studied in the time and frequency domain. Next, the authors performed numerical simulations for vehicle $^1/_2$ and $^1/_4$ models with the parameters of the piezoelectric stack and the car suspension parameters by using MATLAB/Simulink software. The numerical simulation results of the vehicle model $^1/_4$ have been verified experimentally under harmonic excitation. The results show good agreement with the simulation results at different frequencies of excitation. Therefore, this paper focuses on studying the system of dynamic vibration absorber with piezoelectric stack energy harvester (DVA-PSEH) installed in the undamped primary system under base excitation

2. UNDAMPED PRIMARY SYSTEM SUBJECTED TO BASE EXCITATION WITH A DYNAMIC VIBRATION ABSORBER

Now we consider the system of the undamped primary system with a conventional DVA subjected to base excitation as shown in Fig. 1(a), and dynamic vibration absorber with mass m_2, damping coefficient c_2, the stiffness k_d as shown in Fig. 1(b). The governing

equations for the system are

$$m_1\ddot{x}_1 - c_2\dot{x}_2 + k_1x_1 - k_dx_2 = -m_1\ddot{z}, \tag{1}$$

$$m_2\ddot{x}_2 + c_2\dot{x}_2 + k_dx_2 = -m_2(\ddot{x}_1 + \ddot{z}), \tag{2}$$

where $z(t)$ is harmonic base excitation, z_0 and Ω are the amplitude and frequency of excitation

$$z(t) = z_0\cos\Omega t, \quad \ddot{z}(t) = z_0\Omega^2\cos\Omega t. \tag{3}$$

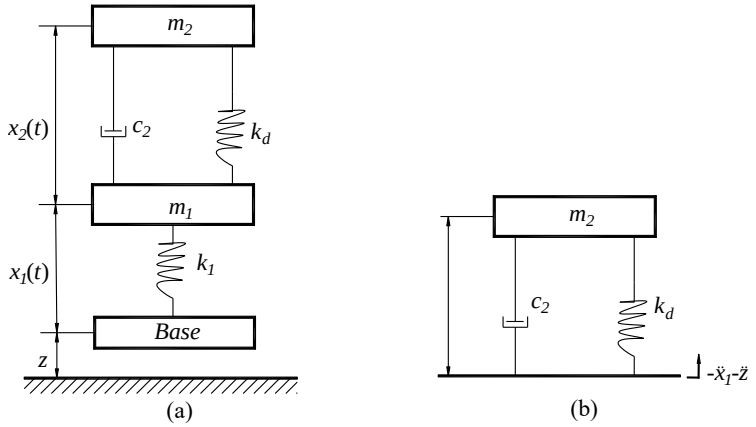

Fig. 1. (a) The primary system with dynamic vibration absorber under base excitation; (b) Dynamic vibration absorber

By setting

$$\mu = \frac{m_2}{m_1}, \quad \omega_1 = \sqrt{\frac{k_1}{m_1}}, \quad \omega_d = \sqrt{\frac{k_d}{m_2}}, \quad \xi_2 = \frac{c_2}{2m_2\omega_d}, \quad \beta = \frac{\omega_d}{\omega_1}, \quad \lambda = \frac{\Omega}{\omega_1}, \tag{4}$$

where μ is the ratio of masses, ω_1 is the natural frequency of the primary system, ω_d, ξ_2, β are the natural frequency, damping and tuning ratios of DVA, respectively; λ is the ratio of excitation frequency to primary system's natural frequency.

The governing equations (1)–(2) can be rewritten as

$$\ddot{x}_1 - 2\mu\omega_d\xi_2\dot{x}_2 + \omega_1^2x_1 - \mu\omega_d^2x_2 = -\ddot{z}, \tag{5}$$

$$\ddot{x}_2 + 2\omega_d\xi_2\dot{x}_2 + \omega_d^2x_2 = -\ddot{x}_1 - \ddot{z}. \tag{6}$$

Consider the harmonic excitation (3) in the complex form

$$z = z_0e^{i\Omega t}. \tag{7}$$

The corresponding complex steady-state solutions of the system (5)–(6) are of the form

$$x_1(t) = X_1e^{i\Omega t}, \quad x_2(t) = X_2e^{i\Omega t}, \tag{8}$$

where X_1, X_2 are complex amplitudes. Substituting (7)–(8) into (5)–(6) and solving the system of equations, the magnification factors K_1 and K_2 of masses m_1 and m_2 are, respectively

$$K_1 = \lambda^2 \sqrt{\frac{\left(\beta^2(1+\mu)-\lambda^2\right)^2 + 4\beta^2\lambda^2(1+\mu)^2\xi_2^2}{\left((1-\lambda^2)(\lambda^2-\beta^2)+\mu\beta^2\lambda^2\right)^2 + 4\beta^2\lambda^2\left(\lambda^2(1+\mu)-1\right)^2\xi_2^2}}, \tag{9}$$

$$K_2 = \frac{\lambda^2}{\sqrt{\left((1-\lambda^2)(\lambda^2-\beta^2)+\mu\beta^2\lambda^2\right)^2 + 4\beta^2\lambda^2(\lambda^2(1+\mu)-1)^2\xi_2^2}}. \tag{10}$$

Applying the fixed-points theory by Den Hartog [10] for the system (5)–(6), the optimal tuning and damping ratios of DVA are given in the form, respectively,

$$\beta_{opt} = \frac{\sqrt{2+\mu}}{\sqrt{2}(1+\mu)}, \tag{11}$$

$$\xi_{2,opt} = \sqrt{\frac{3\mu}{8\,(1+\mu)}}. \tag{12}$$

3. UNDAMPED PRIMARY SYSTEM SUBJECTED TO BASE EXCITATION WITH A DYNAMIC VIBRATION ABSORBER INTEGRATED WITH A PIEZOELECTRIC STACK ENERGY HARVESTING

First, we consider the PSEH governed by constitute equations [9], as shown in Fig. 2(a)

$$f_p = k_p x_p + \theta_p V, \tag{13}$$

$$q = \theta_p x_p - C_p V, \tag{14}$$

where

$$k_p = \frac{E_p A_p}{n h_p}, C_p = n\frac{\varepsilon_{33} A_p}{h_p}, \theta_p = \frac{e_{33} A_p}{h_p}. \tag{15}$$

In (13)–(15), A_p is the section area of the PSEH with n layers, h_p is the thickness of a single piezoelectric layer, E_p is the elastic modulus of piezoelectric material, e_{33} is the piezoelectric stress constant, ε_{33} is the permittivity, f_p is axial force, V is the voltage across the external resistor R, q is electric charge, x_p is deformation, and k_p, θ_p, C_p are stiffness, effective electromechanical coupling coefficient, internal capacitance, respectively.

Fig. 2(b) illustrates the model of the primary system with DVA-PSEH, in which the PSEH is connected in series with the spring of the DVA. In this model, the stiffness of the spring k_d and the stiffness of the piezoelectric stack k_p are equivalently replaced by an equivalent PSEH with the stiffness k_2, electromechanical coupling coefficient θ, and internal capacitance C as depicted in Fig. 2(c) (see [11]). At that time, the governing equations for the electromechanical system are

$$m_1\ddot{x}_1 - c_2\dot{x}_2 + k_1 x_1 - k_2 x_2 - \theta V = -m_1\ddot{z}, \tag{16}$$

$$m_2\ddot{x}_2 + c_2\dot{x}_2 + k_2 x_2 + \theta V = -m_2(\ddot{x}_1 + \ddot{z}), \tag{17}$$

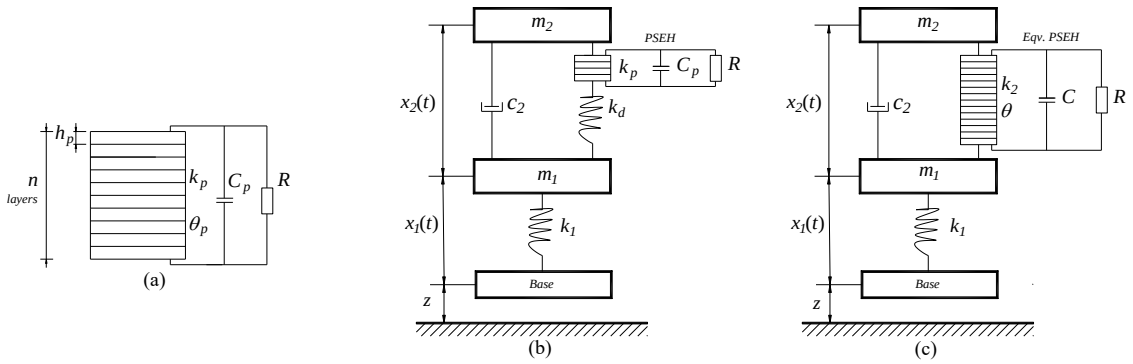

Fig. 2. Schematic of: (a) PSEH; (b) The primary system with DVA-PSEH; (c) The primary system with DVA- equivalent PSEH

$$C\dot{V} + \frac{V}{R} = \theta \dot{x}_2. \tag{18}$$

Let's denote

$$\omega_2 = \sqrt{\frac{k_2}{m_2}}, \quad \hat{\xi}_2 = \frac{c_2}{2m_2\omega_2}, \quad \hat{\beta} = \frac{\omega_2}{\omega_1}, \kappa^2 = \frac{\theta^2}{k_2 C}, \quad \alpha = \frac{1}{\Omega RC}, \quad v = \frac{CV}{\theta}, \tag{19}$$

where κ^2 is the electromechanical coupling coefficient, α is the resistance ratio, and v is the transformed voltage. Then the equation system (16)–(18) is rewritten as

$$\ddot{x}_1 - 2\mu\omega_2\hat{\xi}_2\dot{x}_2 + \omega_1^2 x_1 - \mu\omega_2^2 x_2 - \mu\omega_2^2\kappa^2 v = -\ddot{z}, \tag{20}$$

$$\ddot{x}_2 + 2\omega_2\hat{\xi}_2\dot{x}_2 + \omega_2^2 x_2 + \omega_2^2\kappa^2 v = -\ddot{x}_1 - \ddot{z}, \tag{21}$$

$$\dot{v} + \alpha\Omega v = \dot{x}_2. \tag{22}$$

The corresponding complex steady-state solutions of the system (20)–(22) are of the form

$$\tilde{x}_1(t) = X_1 e^{i\Omega t}, \quad \tilde{x}_2(t) = X_2 e^{i\Omega t}, \quad \tilde{v}(t) = X_v e^{i\Omega t}, \tag{23}$$

where X_1, X_2, X_v are complex amplitudes. Substituting (23) into (20)–(22) leads to

$$(\omega_1^2 - \Omega^2)X_1 - (i2\mu\omega_2\hat{\xi}_2\Omega + \mu\omega_2^2)X_2 - \mu\omega_2^2\kappa^2 X_v = \Omega^2 z_0, \tag{24}$$

$$-\Omega^2 X_1 + (i2\hat{\xi}_2\omega_2\Omega + \omega_2^2 - \Omega^2)X_2 + \omega_2^2\kappa^2 X_v = \Omega^2 z_0, \tag{25}$$

$$-iX_2 + (i + \alpha)X_v = 0. \tag{26}$$

Removing ω_1 from (24)–(25) gives

$$(1 - \lambda^2)X_1 - (i2\mu\hat{\xi}_2\lambda\beta + \mu\beta^2)X_2 - \mu\beta^2\kappa^2 X_v = \lambda^2 z_0, \tag{27}$$

$$-\lambda^2 X_1 + (i2\hat{\xi}_2\lambda\beta + \beta^2 - \lambda^2)X_2 + \beta^2\kappa^2 X_v = \lambda^2 z_0, \tag{28}$$

$$-iX_2 + (i + \alpha)X_v = 0. \tag{29}$$

Solving (27)–(29) gets

$$\frac{X_1}{z_0} = \frac{B_1 + B_2 i}{E_1 + E_2 i}, \quad \frac{X_2}{z_0} = \frac{C_1 + C_2 i}{E_1 + E_2 i}, \quad \frac{X_v}{z_0} = \frac{D_1 + D_2 i}{E_1 + E_2 i}, \tag{30}$$

where

$$\begin{gathered} B_1 = \alpha\lambda^4 + \hat{\beta}\lambda(1+\mu)(2\lambda^2\hat{\xi}_2 - \alpha\hat{\beta}\lambda), \quad B_2 = \lambda^4 - \hat{\beta}\lambda(1+\mu)(\hat{\beta}\lambda(1+\kappa^2) + 2\alpha\lambda^2\hat{\xi}_2), \\ C_1 = \alpha\lambda^2, \quad C_2 = \lambda^2, \quad D_1 = 0, \quad D_2 = \lambda^2, \\ E_1 = \alpha\lambda^2(1-\lambda^2) + \hat{\beta}(1-\lambda^2(1+\mu))(2\lambda\hat{\xi}_2 - \alpha\hat{\beta}), \\ E_2 = \lambda^2(1-\lambda^2) - \hat{\beta}^2(1+\kappa^2) + \hat{\beta}\lambda(1+\mu)(\hat{\beta}\lambda(1+\kappa^2) + 2\alpha\lambda^2\hat{\xi}_2) - 2\alpha\hat{\beta}\lambda\hat{\xi}_2, \end{gathered} \tag{31}$$

Consequently, the steady-state responses of the system (16)–(18) are obtained

$$\begin{aligned} x_1(t) &= a_1 \cos(\Omega t + \varphi_1), \\ x_2(t) &= a_2 \cos(\Omega t + \varphi_2), \\ v(t) &= V_0 \cos(\Omega t + \varphi_v), \end{aligned} \tag{32}$$

where

$$a_1 = |X_1| = z_0\sqrt{\frac{B_1^2 + B_2^2}{E_1^2 + E_2^2}}, \quad \varphi_1 = \tan^{-1}\left(\frac{B_2E_1 - B_1E_2}{B_1E_1 + B_2E_2}\right), \tag{33}$$

$$a_2 = |X_2| = z_0\sqrt{\frac{C_1^2 + C_2^2}{E_1^2 + E_2^2}}, \quad \varphi_2 = \tan^{-1}\left(\frac{C_2E_1 - C_1E_2}{C_1E_1 + C_2E_2}\right), \tag{34}$$

$$V_0 = |X_v| = z_0\sqrt{\frac{D_1^2 + D_2^2}{E_1^2 + E_2^2}}, \quad \varphi_v = \tan^{-1}\left(\frac{D_2E_1 - D_1E_2}{D_1E_1 + D_2E_2}\right). \tag{35}$$

To evaluate the performance of PSEH with the optimal DVA, considering the conditions $\hat{\beta} = \beta_{opt}$ and $\hat{\xi}_2 = \xi_{2,opt}$, namely by substituting (11), (12) in (33)–(35), this will give the magnification factors and voltage amplitude of the optimal DVA with PSEH

$$\begin{aligned} \hat{K}_1 = \frac{a_1}{z_0} = \lambda^2 &\left[\left(\alpha\lambda^2 + (2\lambda\beta_{opt}\xi_{2,opt} - \alpha\beta_{opt}^2)(1+\mu)\right)^2\right. \\ &\left. + \left(\beta_{opt}^2 - \lambda^2 + \beta_{opt}^2(\kappa^2(1+\mu)+\mu) + 2\alpha\lambda\beta_{opt}\xi_{2,opt}(1+\mu)\right)^2\right]^{1/2} \\ &\times \left[\left(\lambda^2(1-\lambda^2) + \beta_{opt}^2(\lambda^2 - \kappa^2 - 1) + \beta_{opt}^2\lambda^2(\kappa^2(1+\mu)+\mu)\right.\right. \\ &\left. +2\alpha\lambda\beta_{opt}\xi_{2,opt}(\lambda^2(1+\mu)-1)\right)^2 \\ &\left. + \left(-\alpha\lambda^2(1-\lambda^2) + (\lambda^2(1+\mu)-1)(2\lambda\beta_{opt}\xi_{2,opt} - \alpha\beta_{opt}^2)\right)^2\right]^{-1/2}, \end{aligned} \tag{36}$$

$$\begin{aligned} \hat{K}_2 = \frac{a_2}{z_0} = \lambda^2(1+\alpha^2)^{1/2} &\\ \times \left[\left(\lambda^2(1-\lambda^2) + \beta_{opt}^2(\lambda^2 - \kappa^2 - 1) + \beta_{opt}^2\lambda^2(\kappa^2(1+\mu)+\mu)\right.\right. &\\ \left. +2\alpha\lambda\beta_{opt}\xi_{2,opt}(\lambda^2(1+\mu)-1)\right)^2 &\\ \left. + \left(-\alpha\lambda^2(1-\lambda^2) + (\lambda^2(1+\mu)-1)(2\lambda\beta_{opt}\xi_{2,opt} - \alpha\beta_{opt}^2)\right)^2\right]^{-1/2}, \end{aligned} \tag{37}$$

$$V_0 = \Big[\Big(\lambda^2(1-\lambda^2) + \beta_{opt}^2(\lambda^2-\kappa^2-1) + \beta_{opt}^2\lambda^2(\kappa^2(1+\mu)+\mu) + 2\alpha\lambda\beta_{opt}\xi_{2,opt}(\lambda^2(1+\mu)-1)\Big)^2 + \Big(-\alpha\lambda^2(1-\lambda^2) + (\lambda^2(1+\mu)-1)(2\lambda\beta_{opt}\xi_{2,opt} - \alpha\beta_{opt}^2)\Big)^2\Big]^{-1/2} z_0\lambda^2. \tag{38}$$

Using (19) and (38), we get the electric power harvested from the DVA-PSEH system

$$\begin{aligned} P_{out} = \frac{V^2}{R} &= \frac{\theta^2}{RC^2}V_0^2\cos^2(\Omega t+\varphi_v) \\ &= \frac{\theta^2}{RC^2}z_0^2\lambda^4\cos^2(\Omega t+\varphi_v) \\ &\quad\times\Big[\Big(\lambda^2(1-\lambda^2) + \beta_{opt}^2(\lambda^2-\kappa^2-1) + \beta_{opt}^2\lambda^2(\kappa^2(1+\mu)+\mu) \\ &\quad + 2\alpha\lambda\beta_{opt}\xi_{2,opt}(\lambda^2(1+\mu)-1)\Big)^2 \\ &\quad + \Big(-\alpha\lambda^2(1-\lambda^2) + (\lambda^2(1+\mu)-1)(2\lambda\beta_{opt}\xi_{2,opt} - \alpha\beta_{opt}^2)\Big)^2\Big]^{-1}, \end{aligned} \tag{39}$$

or in the dimensionless form

$$\begin{aligned} \frac{P_{out}}{\omega_1^3 m_1 z_0^2} &= \mu\alpha\hat{\beta}^2\kappa^2\lambda^5\cos^2(\Omega t+\varphi_v) \\ &\quad\times\Big[\Big(\lambda^2(1-\lambda^2) + \beta_{opt}^2(\lambda^2-\kappa^2-1) + \beta_{opt}^2\lambda^2(\kappa^2(1+\mu)+\mu) \\ &\quad + 2\alpha\lambda\beta_{opt}\xi_{2,opt}(\lambda^2(1+\mu)-1)\Big)^2 \\ &\quad + \Big(-\alpha\lambda^2(1-\lambda^2) + (\lambda^2(1+\mu)-1)(2\lambda\beta_{opt}\xi_{2,opt} - \alpha\beta_{opt}^2)\Big)^2\Big]^{-1}. \end{aligned} \tag{40}$$

Hence, the dimensionless averaging power determined from (40) is

$$\begin{aligned} P_{av} = \frac{\Omega}{2\pi}\int_0^{2\pi/\Omega}\frac{P_{out}}{\omega_1^3 m_1 z_0^2}\mathrm{d}t &= \frac{1}{2}\mu\alpha\beta^2\kappa^2\lambda^5 \\ &\quad\times\Big[\Big(\lambda^2(1-\lambda^2) + \beta_{opt}^2(\lambda^2-\kappa^2-1) + \beta_{opt}^2\lambda^2(\kappa^2(1+\mu)+\mu) \\ &\quad + 2\alpha\lambda\beta_{opt}\xi_{2,opt}(\lambda^2(1+\mu)-1)\Big)^2 \\ &\quad + \Big(-\alpha\lambda^2(1-\lambda^2) + (\lambda^2(1+\mu)-1)(2\lambda\beta_{opt}\xi_{2,opt} - \alpha\beta_{opt}^2)\Big)^2\Big]^{-1}. \end{aligned} \tag{41}$$

4. RESULTS AND DISCUSSION

In this section, the numerical simulations are implemented for performance analysis of the system (36)–(41) with the corresponding values

$$\mu = 0.05, \quad \alpha = 1, \quad \omega_1 = 1, \quad \kappa^2 = 0.005.$$

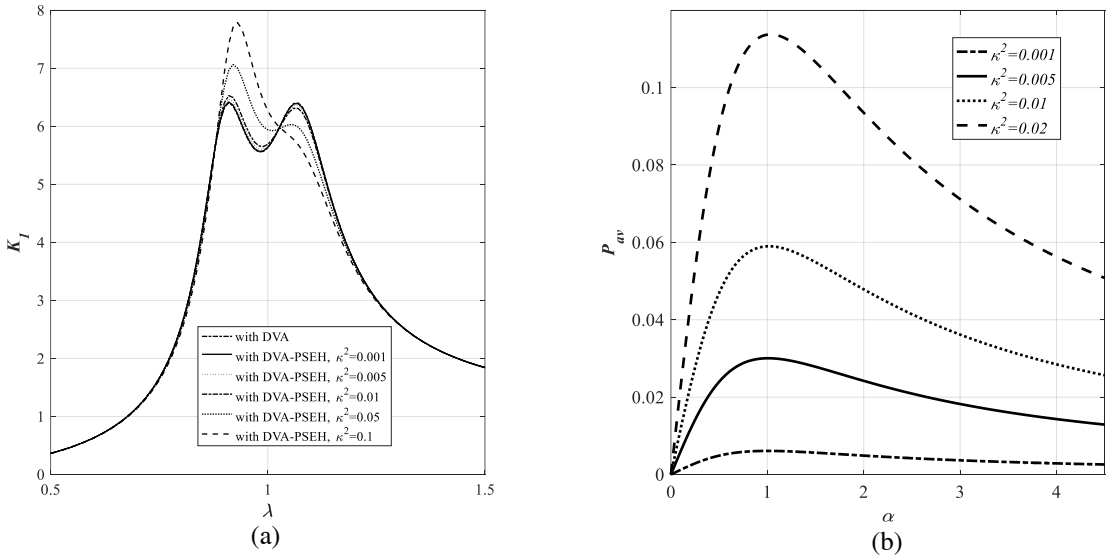

Fig. 3. (a) The magnification factor of the primary system versus λ;
(b) The dimensionless averaging power versus α with various values of κ^2

Fig. 3(a) depicts the magnification factor of the primary system $\hat{K}_1$ versus λ in two combinations: with DVA, and with DVA-PSEH with various values of κ^2. We can see that the optimal DVA helps to reduce significantly the vibration of the primary system with β_{opt} and $\xi_{2,opt}$. When adding a PSEH, the vibration amplitude of the primary system becomes dependent on the electromechanical coupling coefficient κ^2, so the vibration amplitude of the primary system increases with the increase of κ^2. If κ^2 is very small, e.g. $\kappa^2 = 0.001$, then the DVA-PSEH works as a conventional DVA. The two peaks of the vibration amplitude of the primary system occur at $\lambda_1 = 0.93$ and $\lambda_2 = 1.07$.

Fig. 3(b) illustrates the dimensionless averaging power P_{av} of PSEH versus α with various values of κ^2. It is easily seen that the average power increases as κ^2 increases and vice versa. However, as shown in Fig. 3(a), the increase of κ^2 also makes the vibration amplitude of the primary system gets larger. Therefore, for obtaining both purposes of reducing the vibration of the primary system to an acceptable level, and getting the electrical energy as much as possible, κ^2 should be chosen in the interval [0.005, 0.01] corresponding with the above-mentioned input parameters.

Fig. 4(a) describes the dimensionless displacement and voltage responses versus time t. One can observe that the displacement response of DVA-PSEH is out of phase with the displacement response of the primary system, but in phase with the voltage response. This helps to obtain both purposes of the well-designed DVA-PSEH. The graphs of the voltage response corresponding with two peak frequencies, i.e. $\lambda_1 = 0.93$ and $\lambda_2 = 1.07$, show that the voltage amplitude at the first is larger than at the latter.

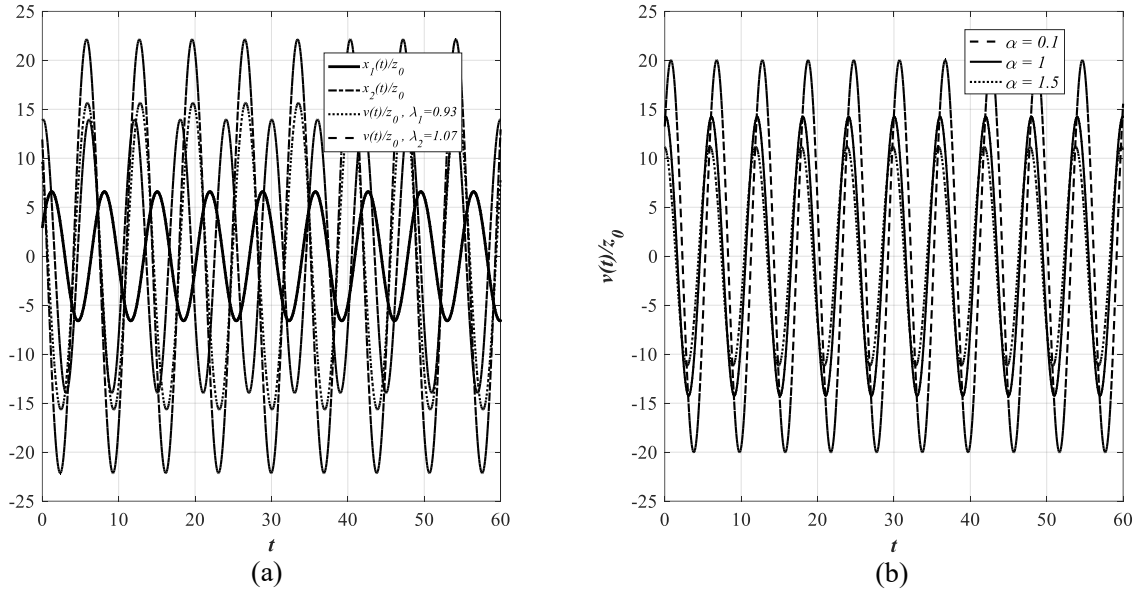

Fig. 4. (a) Dimensionless displacement and voltage responses versus time t; (b) Voltage response with variations of α

Fig. 4(b) shows the time history of the voltage response with various values of α. As we can see, the voltage amplitude is larger as the value of α is in the interval [0, 1], but smaller as $\alpha > 1$. Thus, for better harvested voltage, the value of α should be chosen in the vicinity of 1.

5. CONCLUSIONS

First, Den Hartog's fixed point theory is used to determine the optimal coefficients of a conventional dynamic vibration absorber mounted on the primary system subjected to base excitation. Next, the equivalent replacement is used to replace the series combination of spring and piezoelectric stack in the dynamic vibration absorber with an equivalent PSEH having stiffness k_2, electromechanical coupling coefficient θ, and internal capacitance C. This equivalent PSEH then is used to establish the governing equations for the electromechanical system of DVA-PSEH attached to an undamped primary system subjected to base excitation. Next, the complex amplitude method is used to determine the mechanical and electrical responses of the electromechanical system.

Numerical simulation is carried out. The results show that the electromechanical system dealing with the optimal DVA not only reduces vibrations similar to a conventional system without PSEH, but also efficiently converts vibration energy into electric energy with appropriate values of the electromechanical coupling coefficient κ^2 and the resistance ratio α.

DECLARATION OF COMPETING INTEREST

The authors declare that they have no known competing financial interests or personal relationships that could have appeared to influence the work reported in this paper.

ACKNOWLEDGMENT

The authors would like to sincerely thank the reviewers, the organizing committee of the NACOME 2022, and the Editor Board of the Vietnam Journal of Mechanics, for their valuable comments and support that helped us improve our work. This paper is supported by Vietnam Academy of Sciences and Technology under code NCVCC 2022-2023.

REFERENCES

[1] A. Erturk and D. J. Inman. *Piezoelectric energy harvesting*. Wiley, (2011). https://doi.org/10.1002/9781119991151.

[2] M. Goldfarb and N. Celanovic. Modeling piezoelectric stack actuators for control of micromanipulation. *IEEE Control Systems*, **17**, (1997), pp. 69–79. https://doi.org/10.1109/37.588158.

[3] J. Feenstra, J. Granstrom, and H. Sodano. Energy harvesting through a backpack employing a mechanically amplified piezoelectric stack. *Mechanical Systems and Signal Processing*, **22**, (2008), pp. 721–734. https://doi.org/10.1016/j.ymssp.2007.09.015.

[4] F. Qian, T.-B. Xu, and L. Zuo. Design, optimization, modeling and testing of a piezoelectric footwear energy harvester. *Energy Conversion and Management*, **171**, (2018), pp. 1352–1364. https://doi.org/10.1016/j.enconman.2018.06.069.

[5] X. Jiang, Y. Li, J. Li, J. Wang, and J. Yao. Piezoelectric energy harvesting from traffic-induced pavement vibrations. *Journal of Renewable and Sustainable Energy*, **6**, (2014). https://doi.org/10.1063/1.4891169.

[6] W. Hendrowati, H. L. Guntur, and I. N. Sutantra. Design, modeling and analysis of implementing a multilayer piezoelectric vibration energy harvesting mechanism in the vehicle suspension. *Engineering*, **04**, (11), (2012), pp. 728–738. https://doi.org/10.4236/eng.2012.411094.

[7] T. Darabseh, D. Al-Yafeai, A.-H. I. Mourad, and F. Almaskari. Piezoelectric method-based harvested energy evaluation from car suspension system: Simulation and experimental study. *Energy Science & Engineering*, **9**, (2020), pp. 417–433. https://doi.org/10.1002/ese3.829.

[8] J. Wang, Z. Shi, H. Xiang, and G. Song. Modeling on energy harvesting from a railway system using piezoelectric transducers. *Smart Materials and Structures*, **24**, (2015). https://doi.org/10.1088/0964-1726/24/10/105017.

[9] Y.-A. Lai, J.-Y. Kim, C.-S. W. Yang, and L.-L. Chung. A low-cost and efficient d33-mode piezoelectric tuned mass damper with simultaneously optimized electrical and mechanical tuning. *Journal of Intelligent Material Systems and Structures*, **32**, (2020), pp. 678–696. https://doi.org/10.1177/1045389x20966056.

[10] J. P. D. Hartog. *Mechanical vibrations*. New York: McGraw-Hill, (1956).

[11] N. N. Linh. Series combination models of piezoelectric energy harvesters with spring and damper. In *the 11th National Conference on Mechanics*, Vol. 2. (in Vietnamese).